Arch. Pharm. Chem. Life Sci. 2015, *348*, 366–374

ARCH PHARM
Archiv der Pharmazie

Full Paper

9*H*-Carbazole Derivatives Containing the *N*-Benzyl-1,2,3-triazole Moiety as New Acetylcholinesterase Inhibitors

Hamidreza Akrami[1,2], Bibi F. Mirjalili[2], Mehdi Khoobi[1], Alireza Moradi[3], Hamid Nadri[3], Saeed Emami[4], Alireza Foroumadi[1], Mohsen Vosooghi[1], and Abbas Shafiee[1]

[1] Department of Medicinal Chemistry, Faculty of Pharmacy and Pharmaceutical Sciences Research Center, Tehran University of Medical Sciences, Tehran, Iran
[2] Department of Chemistry, College of Science, Yazd University, Yazd, Iran
[3] Faculty of Pharmacy, Shahid Sadoughi University of Medical Sciences, Yazd, Iran
[4] Department of Medicinal Chemistry and Pharmaceutical Sciences Research Center, Faculty of Pharmacy, Mazandaran University of Medical Sciences, Sari, Iran

A series of triazole-containing carbazole derivatives were designed as new anti-acetylcholinesterase (AChE) agents. The target compounds **6a–q** were simply prepared via a one-pot three-component click reaction of *N*-propargyl-9*H*-carbazole, sodium azide, and an appropriate benzyl halide. The *in vitro* anti-cholinesterase assay showed that the unsubstituted benzyl derivative **6p** along with the 2-F, 2-Me, 3-Me, 3-MeO, and 3-F analogs (**6a**, **6c**, and **6g–i**) had significant anti-AChE activity (IC_{50}s $\leq 3.8\,\mu M$). Among them, the 2-methylbenzyl derivative **6c** with an IC_{50} value of $1.9\,\mu M$ was the most active compound. The SAR studies revealed that small halogen atoms such as the fluorine atom or electron-donating groups such as methyl or methoxy at the *ortho* or *meta* positions of the benzyl pendent group could be tolerated or improved the anti-AChE activity.

Keywords: Acetylcholinesterase / Alzheimer's disease / Click chemistry / Docking study / 9*H*-Carbazole / Triazole

Received: September 27, 2014; Revised: February 2, 2015; Accepted: February 6, 2015

DOI 10.1002/ardp.201400365

Additional supporting information may be found in the online version of this article at the publisher's web-site.

Introduction

Alzheimer's disease (AD) is a chronic, irreversible, and progressive neurodegenerative disorder that produces severe cognitive impairment in elderly individuals. Although, the early stages of AD associate with mild cognitive decline and progressive memory loss, at the late stages patients exhibit personality alteration and consumption of bodily functions [1]. AD is the main neurological cause of dementia and is a growing health crisis around the world. Currently, 38 million people suffer from AD worldwide, elderly adults in most cases [2]. It is estimated that those numbers will approximately double every 20 years and reach 115 million in 2050 [3].

At the molecular level, AD is characterized by the presynaptic decrease of acetylcholine (ACh), extracellular deposition of amyloid-β (Aβ) plaques, and intracellular accumulation of hyper-phosphorylated tau protein and neurofibrillary tangles (NFTs) [1]. Although remarkable development has been made at the present time in our data about AD pathogenesis, there is still no effective treatment to mitigate the neurological deficits associated with AD or to prevent the disease. Currently, patients suffering from AD may be treated with approved acetylcholinesterase (AChE) inhibitors such as rivastigmine, donepezil, and galantamine (**I**). However, AChE inhibitors ameliorate the symptoms of AD, but the clinical efficacy of them is considered to be very limited [4].

Correspondence: Dr. Abbas Shafiee, Department of Medicinal Chemistry, Faculty of Pharmacy and Pharmaceutical Sciences Research Center, Tehran University of Medical Sciences, Tehran 14176, Iran.
E-mail: ashafiee@ams.ac.ir
Fax: +98 21 66461178

Carbazoles are naturally occurring phytochemicals which possess a wide range of biological activities including beneficial effect in AD [5]. A study by Yang et al. [6] showed that carbazole derivatives have the capacity of inhibiting Aβ aggregation. Moreover, the substituted carbazole derivative carvedilol (**II**) was an effective inhibitor of Aβ fibril formation [7]. Recently, Fang et al. [8] described a series of carbazole derivatives, which can be considered as the D-ring opened analogs of galantamine (**I**). Among these compounds, analog **III** (Fig. 1) showed a potent inhibition activity toward AChE [8]. According to these reports, the carbazole scaffold emerges as attractive building block in the search of new agents to confront AD.

The azide–alkyne cycloaddition reaction or click chemistry has found increasing applications in all aspects of drug development and discovery especially in lead finding [9, 10]. The application of click chemistry in the field of AChE inhibitors has been reported by Sharpless et al. [11, 12]. The X-ray crystallographic studies of 1,2,3-triazole containing AChE inhibitors and mouse AChE suggested that the 1,2,3-triazole moiety of these compounds was involved in van der Waals contact with the Phe297 and Tyr341 side chains [11]. Also, triazole-containing berberine derivatives were prepared via click chemistry and evaluated as AChE and Aβ aggregation inhibitors [13]. Therefore, based on pharmacophoric role of both carbazole and 1,2,3-triazole scaffold, it was desirable to design triazole-containing carbazole derivatives for pharmacological studies in the field of AD therapy. Herein, we report synthesis and biological evaluation of 9-((1-benzyl-1*H*-1,2,3-triazol-4-yl)methyl)-9*H*-carbazole derivatives as new AChE inhibitors.

Results and discussion

Chemistry

As illustrated in Scheme 1, target compounds **6a–q** were easily synthesized in two steps. At first, 9-(prop-2-yn-1-yl)-9*H*-carbazole (**3**) was synthesized via the reaction between carbazole (**1**) and propargyl bromide (**2**). Several bases and solvents were screened for this reaction, but the best result was obtained in the presence of sodium hydride (NaH) as a base and a mixture of DMF and THF as solvent at ambient temperature. Finally, copper-catalyzed azide–alkyne cycloaddition (CuAAC) was used to prepare the novel carbazole derivatives **6** bearing *N*-benzyl triazole moiety via one-pot three-component click reaction of alkyne **3**, sodium azide (**4**), and benzyl halides **5**. All of target compounds were obtained as pure 1,4-substituted regioisomers and isolated by simple crystallization from ethanol without the need for chromatography. Combination of Cu(II) and sodium ascorbate has been used as efficient catalyst for regioselective formation of 1,2,3-triazole derivatives by click reaction. In this reaction, sodium ascorbate can act as reducing agent to prevent the formation of oxidative homocoupling products as well as conversion of Cu(II) to Cu(I) [14, 15]. Herein, we checked several Cu(I) or Cu(II) salts using sodium ascorbate and solvents to find the best media (see Supplementary Material). According to the results, the best media were achieved by

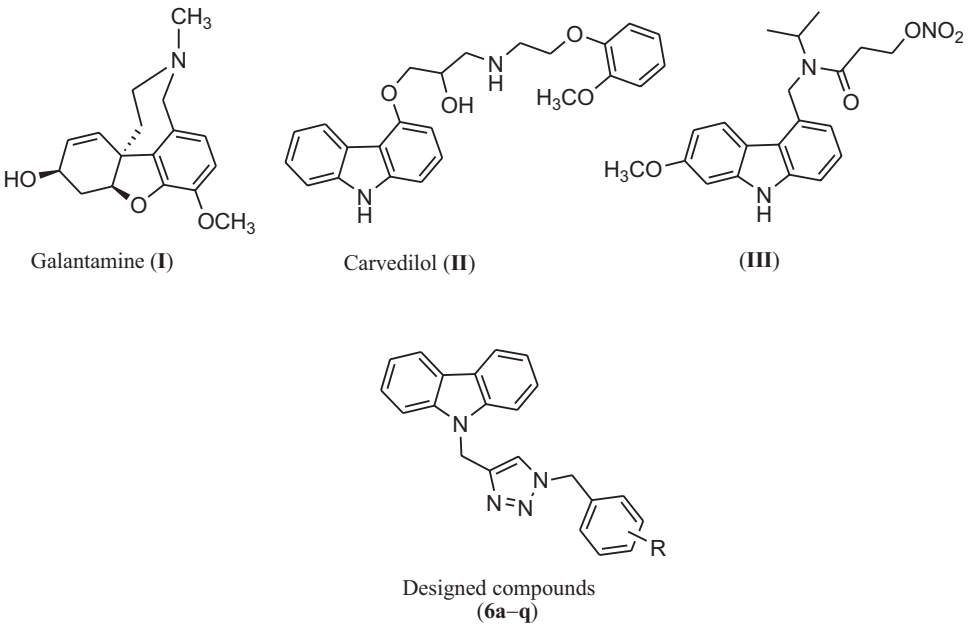

Figure 1. Structures of compounds **I–III** known as useful agents in AD treatment and the new designed compounds **6a–q**.

ARCH PHARM
Archiv der Pharmazie

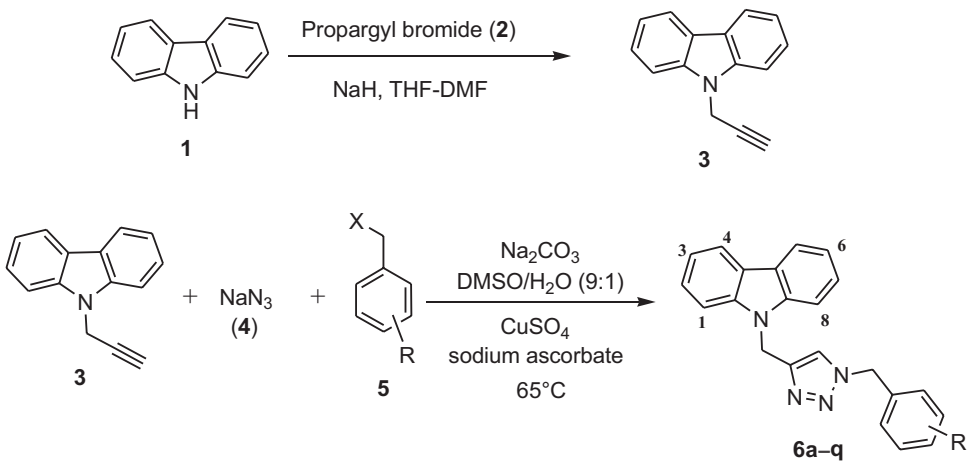

Scheme 1. Synthesis of 9-((1-benzyl-1*H*-1,2,3-triazol-4-yl)methyl)-9*H*-carbazole derivatives **6a–q**.

using mixture of DMSO/water as solvent and sodium ascorbate/$CuSO_4 \cdot 5H_2O$ as catalyst.

Anti-cholinesterase activity

The anti-cholinesterase activity of title compounds **6a–q** was evaluated *in vitro* against AChE in comparison to standard drug tacrine. It should be noted that the fish enzyme from *Electrophorus electricus* (electric eel AChE) was used due to lower price, availability, and high relevance to human AChE. Electric eel AChE and human AChE show high overall sequence homology (56.57%) and 100% amino acid identity in the catalytic triad (http://www.uniprot.org/). The inhibitory activities of compounds against electric eel AChE were expressed as IC_{50} values in Table 1. The results revealed that all compound with the exception of 4-nitrobenzyl derivative **6n** showed significant anti-AChE activity (IC_{50} values = 1.93–27.4 μM). Among the tested compounds, 2-methylbenzyl derivative **6c** with IC_{50} value of 1.93 μM was the most active compound.

As seen in Table 1, the type and position of substitution on the benzyl moiety affected the anti-AChE activity. Although the unsubstituted derivative **6p** showed good activity against AChE (IC_{50} = 3.5 μM), the introduction of substituent on the *para* position diminished the activity as observed in compounds **6j–n** (IC_{50} values = 9.0 to >100 μM). This may be due to the steric effect of *para* substituent on the benzyl moiety. However, the substituent at *ortho* or *meta* positions could slightly improve inhibitory activity. The 2-F, 2-Me, 3-Me, and 3-MeO derivatives (**6a**, **6c**, **6g**, and **6h**, respectively) were more potent than the unsubstituted analog **6p**. No difference was observed between 3-F derivative **6i** and compound **6p**. Thus, 3-fluoro group on the benzyl moiety is tolerated, but could not improve the activity. It is worthwhile to note that the introduction of 2-chloro group diminished the activity (**6b** vs. **6p**), whereas the insertion of fluorine on the *ortho* position of **6b** resulted in 2-chloro-6-fluoro compound **6e** with better activity. As observed with 2- or 4-substituted compounds, the electron withdrawing nitro group decreased the inhibitory activity. The fluorine at *ortho* and *meta* positions was more favorable than chlorine, but the fluorine and chlorine at *para* position had same effect. The comparison of 4-chloro derivative **6k** with 2,4-dichloro compound **6o** revealed that the insertion of second chlorine atom at *ortho* position increased anti-AChE activity. The same IC_{50} values of compounds **6g** and **6h** demonstrated that the 3-methyl and 3-methoxy had equal effect on activity. Also, in the *para*-substituted series, the methoxy substituent was better than halo or nitro groups. Overall, the methyl substituent at *ortho* or *meta* position was the most favorable group for AChE inhibition.

The inhibitory activity of target compounds was screened against equine BuChE. As seen in Table 1, all compounds showed no activity against BuChE (IC_{50} values >100 μM). Thus, the designed compounds are selective inhibitors of AChE.

Kinetic study of AChE inhibition

The representative compound **6c** was subjected to kinetic study to determine its mode of inhibition against AChE. Ellman's procedure was used to construct Lineweaver–Burk double reciprocal plots. The relative velocity (v) of the enzyme was measured using various concentrations of the substrate [S] in the presence and absence of inhibitor. After incorporating of substrate, progress curves have been monitored at 412 nm for just 6 min. Then, $1/v_{max}$ versus 1/[S] was constructed using slopes associated with progress curves to determine the type of inhibition. To obtain the inhibitory constant, slopes of this reciprocal plot were plotted against the concentration of the inhibitor. In the Lineweaver–Burk plot, the interception of the lines above the x-axis (Fig. 2) demonstrated that **6c** can serve as mixed-type inhibitor of AChE. The estimated inhibition constant (K_i) for compound **6c** was 1.31 μM (Fig. 3).

Table 1. The inhibitory activities (IC_{50}s, μM) of synthesized compounds 6a–q against cholinesterases.

Compound	R	IC_{50} (μM) AChE[a),b)]	IC_{50} (μM) BuChE[a),b)]
6a	2-F	2.52 ± 0.10	>100
6b	2-Cl	13.44 ± 0.82	>100
6c	2-Me	1.93 ± 0.11	>100
6d	2-NO_2	21.40 ± 1.02	>100
6e	2-Cl-6-F	4.15 ± 0.31	>100
6f	3-Cl	23.12 ± 1.57	>100
6g	3-Me	2.25 ± 0.19	>100
6h	3-MeO	2.25 ± 0.10	>100
6i	3-F	3.80 ± 0.34	>100
6j	4-F	25.30 ± 1.87	>100
6k	4-Cl	25.20 ± 1.36	>100
6l	4-Br	27.40 ± 1.53	>100
6m	4-MeO	9.00 ± 0.87	>100
6n	4-NO_2	>100	>100
6o	2,4-Cl_2	20.80 ± 0.93	>100
6p	H	3.50 ± 0.33	>100
6q	4-Me	12.20 ± 0.95	>100
Tacrine		0.41 ± 0.018	0.35 ± 0.025

[a)] The concentration of inhibitor required to produce 50% enzyme inhibition.
[b)] Data are means of triplicate independent experiments.

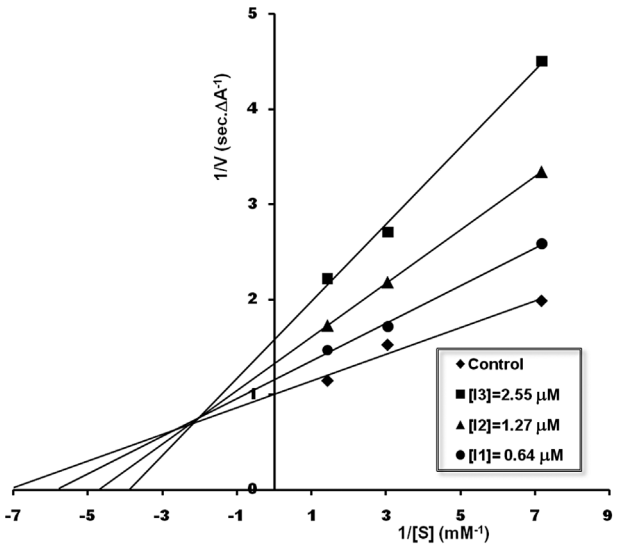

Figure 2. Lineweaver–Burk plots showing mixed-type inhibition of AChE by compound **6c**.

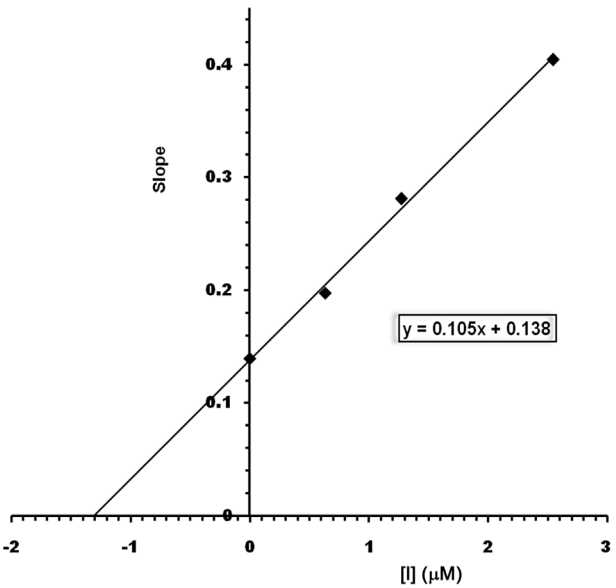

Figure 3. Determination of K_i value for most active derivative **6c** by re-plotting slopes of lines from the Lineweaver–Burk plot versus the inhibitor concentrations.

Ligand–protein docking simulation

The docking study was performed to comprehend the binding interactions. The orientation of the most active compound in the gorge of the enzyme was represented in Fig. 4. The docking results revealed that the compound **6c** could interact with the catalytic anionic subsite (CAS) and the peripheral anionic binding site (PAS) of the enzyme as well. Regarding the hydrophobic nature of the compound **6c**, the hydrophobic interactions play an important role in the binding. The compound fits in the gorge of the enzyme and occupies the cavity between CAS and PAS. In the neighborhood of catalytic triad, the carbazole moiety makes a π–π interaction with Trp84 of CAS. The rest of the molecule leans over the PAS by making a further π–π interaction between triazole ring and

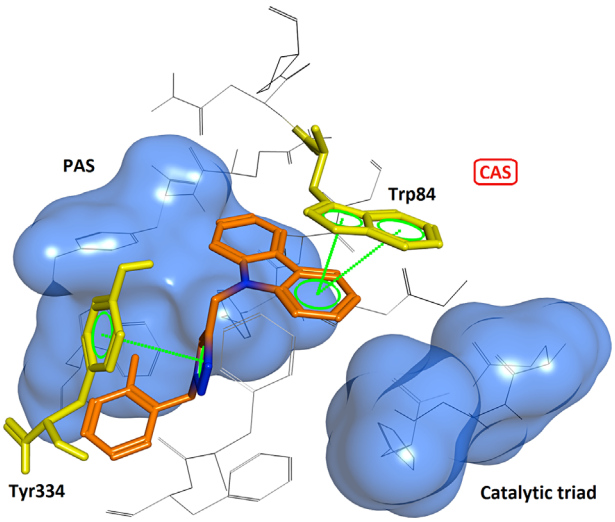

Figure 4. Schematic interaction of compound **6c** with the active site of AChE. π–π interactions are represented as green dashed lines.

Tyr334. In this position, the substituted phenyl ring fits in the hydrophobic pocket composed by Trp279 and Tyr70.

Furthermore, the potent carbazole analog **III** (Fig. 1) as a lead compound and tacrine as a reference drug was subjected to docking study to compare with representative compound **6c**. As illustrated in Fig. 5, the tricyclic part of all molecules was located at the bottom of active site in the vicinity of catalytic triad. The hydrophobic planar nature of tricyclic moiety allows making more favorable sandwich π stacking with Phe330 and Trp84. The hydrophobic pendant part of compound **6c** lies along the gorge to interact with PAS. On the other hand, the hydrophilic tail of compound **III** rotates toward Ser122 to make a hydrogen bond.

As mentioned above, by using click reaction, we prepared prototype compound **6c**, as 1,4-substituted 1,2,3-triazole analog. One might think that an 1,5-disubstituted regioisomer of compound **6c** could be also potent inhibitor of AchE. Accordingly, the 1,5-regioisomer of the most potent compound **6c** was subjected to docking study in order to evaluate the binding mode and potential activity. As shown in Fig. 6, the binding mode of 1,4- and 1,5-regioisomers was different in terms of binding interactions, as well as binding energy. The calculated free binding energy of 1,4- and 1,5-regioisomers was 12.1 and 11.3 kcal/mol, respectively. Therefore, it could be concluded that 1,4-regioisomer would be the more active inhibitor.

Conclusion

We designed triazole-containing carbazole derivatives as new anti-AChE agents. The title compounds namely 9-((1-benzyl-1*H*-1,2,3-triazol-4-yl)methyl)-9*H*-carbazoles were simply prepared

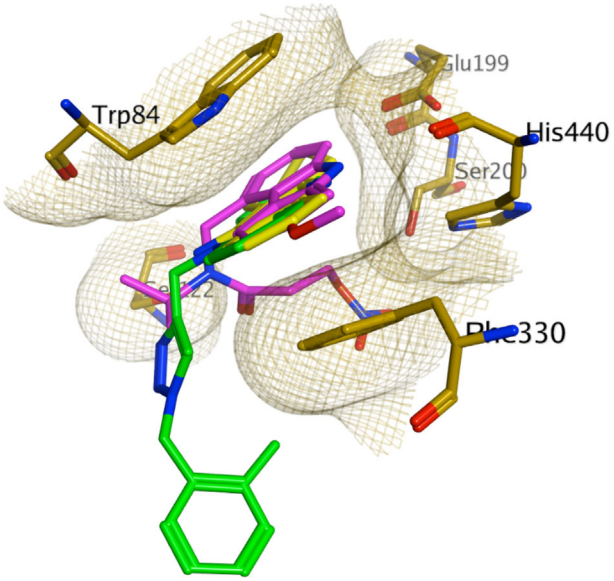

Figure 5. Overlay of the most favorable docked conformations of the most active compound **6c** (green), compound **III** (magenta), and tacrine (yellow) in the active sites of AChE (brown).

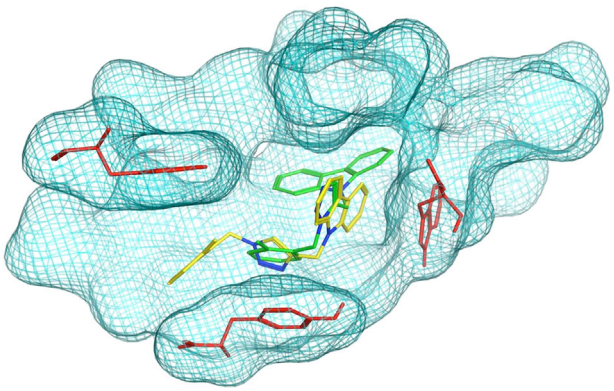

Figure 6. The 1,5-regioisomer of compound **6c** (green) overlaid on compound **6c** (yellow); docked ligands did not show the same binding mode.

via one-pot three-component click reaction of *N*-propargyl-9*H*-carbazole, sodium azide, and appropriate benzyl halide. All compounds with the exception of 4-nitrobenzyl derivative showed anti-AChE activity. The 2-methylbenzyl derivative **6c** with IC_{50} value of 1.93 μM was the most active compound against AChE. The SAR studies revealed that the substituent at the *para* position of benzyl moiety diminished the activity, whereas small halogen such as fluorine atom or electron-donating groups such as methyl or methoxy at the *ortho* or *meta* positions of benzyl pendent group could be tolerated or

improved the anti-AChE activity. Since the target compounds showed no activity against BuChE, the prototype **6** could be considered as selective AChE inhibitors.

Experimental

Chemistry

All commercially available reagents were purchased from Merck AG or Aldrich and used without further purification. TLC was conducted on silica gel 250 μm. Melting points were measured on the Buchi Melting point B-540. FT-IR spectra were run on a Bruker, Eqinox 55 spectrometer (ATR). Mass spectra of the products were obtained with an HP (Agilent Technologies) 5937 mass selective detector. ^{1}H NMR spectra were recorded on a Bruker 400 MHz NMR instrument. The chemical shifts (δ) and coupling constants (J) are expressed in parts per million and Hertz, respectively. The atoms numbering of the target compounds used for ^{1}H NMR data has been shown in Scheme 1. Elemental analyses were carried out by a CHN-Rapid Heraeus elemental analyzer. The results of elemental analyses (C, H, N) were within ±0.4% of the calculated values.

*Preparation of 9-(prop-2-yn-1-yl)-9H-carbazole (**3**)*

A solution of carbazole (**1**, 1 mmol) in dry DMF (2 mL) and anhydrous THF (8 mL) were added dropwise into the dried three-necked balloon containing sodium hydride (3 mmol), under an argon atmosphere. Within 10 min, propargyl bromide (**2**, 1.5 mmol) were added dropwise to the reaction mixture. The mixture was kept at room temperature under argon atmosphere for 4.5 h and then neutralized with 15% HCl solution. After extraction with dichloromethane, the organic phase was evaporated and concentrated under vacuum. Then, the residue was dissolved in DMF (1 mL) and brine was added to precipitate a solid. It was filtered, dried (oven, 80°C), and used without further purification. Cream solid; yield 71%; mp 105–107°C; IR (cm^{-1}): 3264, 2923, 1626, 1610, 1595, 1485; ^{1}H NMR (400 MHz, $CDCl_3$) δ: 8.11–8.09 (bs, 2H, $H_{4,5}$), 7.50–7.49 (bs, 2H, $H_{1,8}$), 7.28–7.26 (bs, 4H, $H_{2,3,6,7}$), 5.06 (s, 2H, CH_2), 2.25 (s, 1H, CH). Anal. calcd. for $C_{15}H_{11}N$ (205.25): C, 87.77; H, 5.40; N, 6.82. Found: C, 88.11; H, 5.74; N, 6.54.

*General procedure for the preparation of compounds **6a–q***

In a tube was placed 9-(prop-2-yn-1-yl)-9*H*-carbazole (**3**) (1 mmol) and 3 mL of DMSO/H_2O (9:1). Then, benzyl halide derivative (1.5 mmol), Na_2CO_3 (0.3 mmol), NaN_3 (1.4 mmol), sodium ascorbate (0.2 mmol), and $CuSO_4{\cdot}5H_2O$ (1 mL, 1 M) were added to the mixture. Then, the tube was capped with a septum and the mixture was stirred at 65°C for 15–48 h. When the reaction was completed (monitored by TLC), water (5 mL) was added to the mixture and stirred for 0.5 h. Then, the mixture was extracted with dichloromethane. After evaporation of volatile solvent, ethanol (5 mL) was added to the mixture and the resulting solid was filtrated. The solid product was recrystallized from ethanol to give pure compounds **6a–q**.

*9-((1-(2-Fluorobenzyl)-1H-1,2,3-triazol-4-yl)methyl)-9H-carbazole (**6a**)*

White solid; yield 86%; mp 181–182°C; IR (ATR, cm^{-1}): 3063, 1595, 1486, 1451; ^{1}H NMR (500 MHz, $CDCl_3$) δ: 8.14 (d, J = 7.7 Hz, 2H, $H_{4,5}$), 8.06 (s, 1H, H-triazole), 7.75 (d, J = 8.2 Hz, 2H, $H_{1,8}$), 7.46–7.43 (m, 2H, $H_{2,7}$), 7.39–7.37 (m, 1H, Ar H_3), 7.26–7.14 (m, 5H, $H_{3,6}$, and Ar $H_{4,5,6}$), 5.66 (s, 2H, C$\underline{H}_2$Ar), 5.56 (s, 2H, N–C$\underline{H}_2$). ^{13}C NMR ($CDCl_3$, 125 MHz) δ: 143.8, 140.3, 140.2, 131.1, 131.0, 126.1, 125.2, 123.8, 122.6, 120.6, 119.4, 116.1, 115.9, 110.0, 47.2, 38.0. Anal. calcd. for $C_{22}H_{17}FN_4$ (356.40): C, 74.14; H, 4.81; N, 15.72. Found: C, 74.38; H, 4.60; N, 15.95.

*9-((1-(2-Chlorobenzyl)-1H-1,2,3-triazol-4-yl)methyl)-9H-carbazole (**6b**)*

White solid; yield 85%; mp 142–144°C; IR (ATR, cm^{-1}): 3068, 1595, 1485, 1460; ^{1}H NMR (500 MHz, $CDCl_3$) δ: 8.13–8.07 (m, 3H, $H_{4,5}$, and H-triazole), 7.75 (bs, 2H, $H_{1,8}$), 7.45–7.07 (m, 8H, $H_{2,3,6,7}$, and Ar-$H_{3,4,5,6}$), 5.67 (s, 2H, C$\underline{H}_2$Ar), 5.60 (s, 2H, N–C$\underline{H}_2$). ^{13}C NMR ($CDCl_3$, 125 MHz) δ: 143.7, 140.2, 130.8, 130.6, 130.0, 128.0, 126.1, 124.1, 122.6, 120.6, 119.4, 110.1, 47.2, 38.0. Anal. calcd. for $C_{22}H_{17}ClN_4$ (372.85): C, 70.87; H, 4.60; N, 15.03. Found: C, 70.58; H, 4.32; N, 15.36.

*9-((1-(2-Methylbenzyl)-1H-1,2,3-triazol-4-yl)methyl)-9H-carbazole (**6c**)*

White solid; yield 75%; mp 234–236°C; IR (ATR, cm^{-1}): 3073, 1624, 1594, 1484, 1458; ^{1}H NMR (500 MHz, $CDCl_3$) δ: 8.08 (bs, 2H, $H_{4,5}$), 7.44 (bs, 5H, $H_{1,2,7,8}$, and H-triazole), 7.25–6.94 (m, 6H, $H_{3,6}$, and Ar $H_{3,4,5,6}$), 5.59 (s, 2H, C$\underline{H}_2$Ar), 5.35 (s, 2H, N–C$\underline{H}_2$), 2.18 (s, 3H, CH_3). ^{13}C NMR ($CDCl_3$, 125 MHz) δ: 141.2, 139.1, 137.9, 133.4, 132.0, 130.1, 127.7, 127.0, 124.2, 121.5, 120.5, 109.9, 47.2, 38.5, 20.1. Anal. calcd. for $C_{23}H_{20}N_4$ (352.43): C, 78.38; H, 5.72; N, 15.90. Found: C, 78.65; H, 5.36; N, 16.15.

*9-((1-(2-Nitrobenzyl)-1H-1,2,3-triazol-4-yl)methyl)-9H-carbazole (**6d**)*

Cream solid; yield 84%; mp 179–181°C; IR (ATR, cm^{-1}): 3077, 1595, 1527, 1484; ^{1}H NMR (500 MHz, $CDCl_3$) δ: 8.09 (bs, 3H, $H_{4,5}$, and Ar H_3), 7.53–7.49 (m, 6H, $H_{1,2,3,6,7,8}$), 7.27–6.92 (m, 4H, Ar $H_{4,5,6}$, and H-triazole), 5.81 (s, 2H, C$\underline{H}_2$Ar), 5.68 (br s, 2H, N–C$\underline{H}_2$). ^{13}C NMR ($CDCl_3$, 125 MHz) δ: 142.4, 141.1, 135.4, 131.4, 131.2, 130.7, 127.1, 126.4, 124.2, 121.6, 120.6, 115.9, 115.6, 109.9, 46.1, 39.8. Anal. calcd. for $C_{22}H_{17}N_5O_2$ (383.40): C, 68.92; H, 4.47; N, 18.27. Found: C, 68.63; H, 4.08; N, 18.55.

*9-((1-(2-Chloro-6-fluorobenzyl)-1H-1,2,3-triazol-4-yl)-methyl)-9H-carbazole (**6e**)*

White solid; yield 84%; mp 153–155°C; IR (ATR, cm^{-1}): 3048, 1605, 1578, 1484; ^{1}H NMR (500 MHz, $CDCl_3$) δ: 8.11–8.09 (m, 2H, $H_{4,5}$), 7.47 (bs, 4H, $H_{1,2,7,8}$), 7.28–7.19 (m, 5H, $H_{3,6}$, Ar $H_{3,5}$, and H-triazole), 7.03–6.99 (t, J = 8.4 Hz, 1H, Ar H_4), 5.61–5.57 (m, 4H, N–C$\underline{H}_2$, and C$\underline{H}_2$Ar). ^{13}C NMR ($CDCl_3$, 125 MHz) δ: 164.1, 161.5, 141.2, 136.9, 132.5, 132.4, 127.0, 126.9, 124.2, 121.5, 121.3, 120.5, 115.9, 115.6, 110.0, 46.1, 40.0. Anal. calcd. for

$C_{22}H_{16}ClFN_4$ (390.84): C, 67.61; H, 4.13; N, 14.33 Found: C, 67.32; H, 4.38; N, 14.70.

*9-((1-(3-Chlorobenzyl)-1H-1,2,3-triazol-4-yl)methyl)-9H-carbazole (**6f**)*
Cream solid; yield 83%; mp 178–180°C; IR (ATR, cm^{-1}): 3066, 1596, 1484, 1459; ^1H NMR (500 MHz, $CDCl_3$) δ: 8.14–8.12 (m, 3H, $H_{4,5}$, and H-triazole), 7.74 (d, $J = 8.1$ Hz, 2H, $H_{1,8}$), 7.46–7.43 (t, $J = 7.6$ Hz, 2H, $H_{3,6}$), 7.36 (bs, 2H, $H_{2,7}$), 7.30 (s, 1H, Ar H_2), 7.21–7.18 (m, 3H, Ar $H_{4,5,6}$), 5.65 (s, 2H, $C\underline{H}_2Ar$), 5.29 (s, 2H, N–$C\underline{H}_2$). ^{13}C NMR ($CDCl_3$, 125 MHz) δ: 144.0, 140.2, 131.0, 128.5, 128.1, 127.0, 126.1, 123.9, 122.7, 120.6, 119.4, 110.0, 52.3, 38.0. Anal. calcd. for $C_{22}H_{17}ClN_4$ (372.85): C, 70.87; H, 4.60; N, 15.03. Found: C, 70.52; H, 4.92; N, 15.42.

*9-((1-(3-Methylbenzyl)-1H-1,2,3-triazol-4-yl)methyl)-9H-carbazole (**6g**)*
White solid; yield 78%; mp 189–191°C; IR (ATR, cm^{-1}): 2970, 1653, 1597, 1485, 1460; ^1H NMR (400 MHz, $CDCl_3$) δ: 8.09 (bs, 2H, $H_{4,5}$), 7.79 (bs, 2H, $H_{1,8}$), 7.52–7.45 (m, 5H, $H_{2,3,6,7}$, and H-triazole), 7.19–7.10 (m, 2H, Ar $H_{2,5}$), 6.93 (bs, 2H, Ar $H_{4,6}$), 5.93 (s, 2H, $C\underline{H}_2Ar$), 5.45 (s, 2H, N–$C\underline{H}_2$), 2.26 (s, 3H, CH_3). ^{13}C NMR ($CDCl_3$, 100 MHz) δ: 142.1, 139.3, 137.8, 132.9, 132.2, 130.4, 127.5, 127.0, 124.1, 121.6, 120.4, 108.8, 47.1, 38.5, 20.0. Anal. calcd. for $C_{23}H_{20}N_4$ (352.43): C, 78.38; H, 5.72; N, 15.90. Found: C, 78.75; H, 5.96; N, 15.65.

*9-((1-(3-Methoxybenzyl)-1H-1,2,3-triazol-4-yl)methyl)-9H-carbazole (**6h**)*
White solid; yield 79%; mp 151–152°C; IR (ATR, cm^{-1}): 3069, 2959, 1597, 1485, 1459; ^1H NMR (500 MHz, $CDCl_3$) δ: 8.10–8.08 (m, 2H, $H_{4,5}$), 7.46 (s, 4H, $H_{1,2,7,8}$), 7.26–7.14 (m, 4H, $H_{3,6}$ and Ar H_5, and H-triazole), 6.83–6.63 (m, 3H, Ar $H_{2,4,6}$), 5.63 (s, 2H, $C\underline{H}_2Ar$), 5.34 (s, 2H, N–$C\underline{H}_2$), 3.69 (s, 3H, OCH_3). ^{13}C NMR ($CDCl_3$, 125 MHz) δ: 161.1, 141.2, 136.9, 131.2, 127.1, 124.2, 121.5, 121.1, 120.5, 115.4, 114.3, 109.9, 56.3, 55.3, 40.0. Anal. calcd. for $C_{23}H_{20}N_4O$ (368.43): C, 74.98; H, 5.47; N, 15.21. Found: C, 74.72; H, 5.76; N, 15.45.

*9-((1-(3-Fluorobenzyl)-1H-1,2,3-triazol-4-yl)methyl)-9H-carbazole (**6i**)*
White solid; yield 85%; mp 180–182°C; IR (ATR, cm^{-1}): 3070, 1595, 1486, 1452; ^1H NMR (500 MHz, $CDCl_3$) δ: 8.12–8.10 (m, 2H, $H_{4,5}$), 7.47 (br s, 4H, $H_{1,2,7,8}$), 7.27 (br s, 4H, $H_{3,6}$ and Ar H_2, and H-triazole), 7.02–6.97 (m, 1H, Ar H_5), 6.92–6.83 (m, 2H, Ar $H_{4,6}$), 5.64 (s, 2H, –$C\underline{H}_2Ar$), 5.41 (s, 2H, –N_9–$C\underline{H}_2$). ^{13}C NMR ($CDCl_3$, 100 MHz) δ: 144.1, 140.3, 140.2, 131.2, 131.0, 128.1, 127.2, 123.9, 122.6, 120.7, 119.4, 116.1, 115.9, 110.0, 47.2, 38.0. Anal. calcd. for $C_{22}H_{17}FN_4$ (356.40): C, 74.14; H, 4.81; N, 15.72. Found: C, 74.49; H, 4.50; N, 15.57.

*9-((1-(4-Fluorobenzyl)-1H-1,2,3-triazol-4-yl)methyl)-9H-carbazole (**6j**)*
White solid; yield 83%; mp 186–187°C; IR (ATR, cm^{-1}): 3063, 1601, 1508, 1483, 1451; ^1H NMR (500 MHz, $CDCl_3$) δ: 8.10–8.08 (m, 2H, $H_{4,5}$), 7.45 (bs, 4H, $H_{1,2,7,8}$), 7.27–7.26 (m, 3H, $H_{3,6}$, and H-triazole), 7.14–7.13 (m, 2H, Ar $H_{2,6}$), 7.00–6.98 (m, 2H, Ar $H_{3,5}$), 5.63 (s, 2H, $C\underline{H}_2Ar$), 5.34 (s, 2H, N–$C\underline{H}_2$). ^{13}C NMR ($CDCl_3$, 125 MHz) δ: 142.4, 141.1, 130.9, 130.8, 127.1, 124.2, 124.1, 121.5, 120.6, 117.3, 117.1, 109.9, 54.6, 40.0. Anal. calcd. for $C_{22}H_{17}FN_4$ (356.40): C, 74.14; H, 4.81; N, 15.72. Found: C, 73.88; H, 4.55; N, 15.98.

*9-((1-(4-Chlorobenzyl)-1H-1,2,3-triazol-4-yl)methyl)-9H-carbazole (**6k**)*
White solid; yield 80%; mp 148–150°C; IR (ATR, cm^{-1}): 3068, 1594, 1484, 1452; ^1H NMR (500 MHz, $CDCl_3$) δ: 8.11 (d, $J = 7.6$ Hz, 2H, $H_{4,5}$), 7.46 (bs, 4H, $H_{1,2,7,8}$), 7.27 (bs, 3H, $H_{3,6}$, and H-triazole), 7.16–7.13 (m, 2H, Ar $H_{3,5}$), 7.08 (d, $J = 7.6$ Hz, 2H, Ar $H_{2,6}$), 5.63 (s, 2H, $C\underline{H}_2Ar$), 5.35 (s, 2H, N–$C\underline{H}_2$). ^{13}C NMR ($CDCl_3$, 100 MHz) δ: 141.1, 135.9, 133.9, 130.39, 130.37, 127.1, 124.2, 121.5, 120.6, 115.9, 115.6, 109.9, 54.5, 40.0. Anal. calcd. for $C_{22}H_{17}ClN_4$ (372.85): C, 70.87; H, 4.60; N, 15.03. Found: C, 70.49; H, 4.28; N, 15.40.

*9-((1-(4-Bromobenzyl)-1H-1,2,3-triazol-4-yl)methyl)-9H-carbazole (**6l**)*
White solid; yield 78%; mp 147–148°C; IR (ATR, cm^{-1}): 3073, 2923, 1594, 1486, 1452; ^1H NMR (500 MHz, $CDCl_3$) δ: 8.14 (d, $J = 7.4$ Hz, 2H, $H_{4,5}$), 8.06 (s, 1H, H-triazole), 7.74 (d, $J = 7.9$ Hz, 2H, Ar $H_{3,5}$), 7.53 (d, $J = 8.2$ Hz, 2H, $H_{1,8}$), 7.45 (t, $J = 7.7$ Hz, 2H, $H_{2,7}$), 7.22–7.18 (m, 4H, $H_{3,6}$, and Ar $H_{2,6}$), 5.66 (s, 2H, $C\underline{H}_2Ar$), 5.48 (s, 2H, N–$C\underline{H}_2$). ^{13}C NMR ($CDCl_3$, 125 MHz) δ: 143.9, 140.2, 135.8, 132.0, 130.5, 127.6, 126.1, 123.7, 122.6, 120.6, 119.4, 110.0, 52.4, 38.0. Anal. calcd. for $C_{22}H_{17}ClN_4$ (372.85): C, 70.87; H, 4.60; N, 15.03. Found: C, 70.52; H, 4.28; N, 15.38.

*9-((1-(4-Methoxybenzyl)-1H-1,2,3-triazol-4-yl)methyl)-9H-carbazole (**6m**)*
White solid; yield 77%; mp 147–148°C; IR (ATR, cm^{-1}): 1611, 1514, 1485, 1458; ^1H NMR (500 MHz, $CDCl_3$) δ: 8.11–8.09 (m, 2H, $H_{4,5}$), 7.71 (bs, 4H, $H_{1,2,7,8}$), 7.46 (m, 3H, $H_{3,6}$, and H-triazole), 7.10 (d, $J = 8.0$ Hz, 2H, Ar $H_{2,6}$), 6.82 (d, $J = 8.0$ Hz, 2H, Ar $H_{3,5}$), 4.27–4.18 (m, 7H, $C\underline{H}_2Ar$, N–$C\underline{H}_2$ and –$OC\underline{H}_3$). ^{13}C NMR ($CDCl_3$, 100 MHz) δ: 160.2, 141.1, 136.7, 132.9, 129.3, 127.1, 124.4, 121.5, 120.6, 115.9, 115.6, 109.9, 56.5, 55.4, 40.0. Anal. calcd. for $C_{23}H_{20}N_4O$ (368.43): C, 74.98; H, 5.47; N, 15.21. Found: C, 74.63; H, 5.79; N, 15.53.

*9-((1-(4-Nitrobenzyl)-1H-1,2,3-triazol-4-yl)methyl)-9H-carbazole (**6n**)*
Cream solid; yield 83%; mp 176–178°C; IR (ATR, cm^{-1}): 2925, 1598, 1515, 1485, 1454; ^1H NMR (500 MHz, $CDCl_3$) δ: 8.15–8.11 (m, 6H, $H_{1,4,5,8}$, and Ar $H_{3,5}$), 7.45 (m, 7H, $H_{2,3,6,7}$, and Ar $H_{2,6}$), 5.66 (s, 2H, $C\underline{H}_2Ar$), 5.29 (s, 2H, N–$C\underline{H}_2$). ^{13}C NMR ($CDCl_3$, 100 MHz) δ 142.4, 141.1, 129.6, 127.1, 125.3, 124.9, 124.2, 121.6, 120.7, 115.9, 115.6, 109.8, 54.2, 30.8. Anal. calcd. for $C_{22}H_{17}N_5O_2$ (383.40): C, 68.92; H, 4.47; N, 18.27. Found: C, 68.60; H, 4.79; N, 18.58.

*9-((1-(2,4-Dichlorobenzyl)-1H-1,2,3-triazol-4-yl)methyl)-9H-carbazole (**6o**)*
Cream solid; yield 81%; mp 198–200°C; IR (ATR, cm^{-1}): 3051, 1589, 1484, 1459; ^1H NMR (500 MHz, $CDCl_3$) δ: 8.10 (d, $J = 8.0$ Hz, 2H, $H_{4,5}$), 7.47 (s, 4H, $H_{1,2,7,8}$), 7.38 (s, 1H, H-triazole), 7.27 (br s, 2H, $H_{3,6}$), 7.18 (d, $J = 8.0$ Hz, 1H, Ar H_5), 7.12 (s, 1H, Ar H_3), 6.98 (d, $J = 8.0$ Hz, 1H, Ar H_6), 5.64 (s, 2H, CH_2Ar), 5.45 (s, 2H, N–CH_2). ^{13}C NMR ($CDCl_3$, 100 MHz) δ: 144.2, 139.9, 135.0, 131.3, 130.9, 129.5, 127.7, 122.8, 122.5, 120.3, 119.4, 118.6, 110.9, 109.0, 50.6, 38.5. Anal. calcd. for $C_{22}H_{16}Cl_2N_4$ (407.30): C, 64.88; H, 3.96; N, 13.76. Found: C, 65.12; H, 4.25, N, 13.45.

*9-((1-Benzyl-1H-1,2,3-triazol-4-yl)methyl)-9H-carbazole (**6p**)*
White solid; yield 80%; mp 171–173°C (Ref. [16], mp 177–178); IR (ATR, cm^{-1}): 3050, 1594, 1484, 1450; ^1H NMR (500 MHz, $CDCl_3$) δ: 8.11–8.09 (m, 2H, $H_{4,5}$), 7.46 (bs, 4H, $H_{1,2,7,8}$), 7.30–7.27 (m, 6H, $H_{3,6}$ and Ar $H_{3,4,5}$, and H-triazole), 7.14 (bs, 2H, Ar $H_{2,6}$), 5.63 (s, 2H, –CH_2Ar), 5.41 (s, 2H, –N_9–CH_2). ^{13}C NMR ($CDCl_3$, 125 MHz) δ: 141.2, 135.5, 130.1, 129.8, 129.0, 127.1, 124.2, 121.5, 120.5, 115.9, 115.6, 109.7, 55.5, 39.9. Anal. calcd. for $C_{22}H_{18}N_4$ (338.41): C, 78.08; H, 5.36; N, 16.56. Found: C, 78.39; H, 5.65, N, 16.24.

*9-((1-(4-Methylbenzyl)-1H-1,2,3-triazol-4-yl)methyl)-9H-carbazole (**6q**)*
White solid; yield 86%; mp 150–152°C; IR (ATR, cm^{-1}): 1605, 1535, 1485, 1451; ^1H NMR (500 MHz, $CDCl_3$) δ: 7.97 (br s, 3H, $H_{4,5,8}$), 7.65–7.54 (m, 3H, $H_{1,2,7}$), 7.36 (br s, 3H, $H_{3,6}$ and H-triazole), 7.13–7.02 (m, 4H, Ar $H_{2,3,5,6}$), 5.51 (s, 2H, CH_2Ar), 5.30 (s, 2H, N_9–CH_2), 2.21(s, 3H, –Me). ^{13}C NMR ($CDCl_3$, 125 MHz) δ: 142.8, 139.7, 135.5, 131.7, 128.0, 125.9, 125.2, 123.1, 122.4, 120.3, 119.1, 110.0, 51.5, 39.4, 26.4. Anal. calcd. for $C_{23}H_{21}N_4$ (353): C, 78.16; H, 5.99; N, 15.85. Found: C, 78.40; H, 5.72; N, 15.49.

In vitro inhibition assay for cholinesterases

Acetylcholinesterase (AChE, E.C. 3.1.1.7, type V-S, lyophilized powder, from electric eel, 1000 units), butyrylcholinesterase (BuChE, E.C. 3.1.1.8, from equine serum), and butyrylthiocholine iodide (BTCh) were provided from Sigma–Aldrich. 5,5′-Dithiobis-(2-nitrobenzoic acid) (DTNB) and acetylthiocholine iodide (ATCh) were purchased from Fluka. The inhibition potential of the synthesized compounds was determined using the previously described spectrophotometric process [17]. Briefly, five diverse concentrations of the compounds have been analyzed to obtain 20–80% enzyme inhibition. To prepare stock solutions, the synthesized compounds were dissolved in the absolute ethanol and then diluted in the buffer to make test concentrations. The maximum final concentration of ethanol was 0.15%. The assay solution was composed of 3 mL phosphate buffer (0.1 M, pH = 8), 100 μL DTNB (0.1 M), 50 μL test compound, and 50 μL of 5 IU/mL acetylcholinesterase solution. The above mixture was being pre-incubated for 10 min accompanied by the addition of ATCh (0.15 M, 10 μL). Assays have also been carried out with a blank comprising all ingredients excluding enzyme to consider the non-enzymatic reaction. The absorbance changes have been scored in 412 nm for 6 min and the IC_{50} values have been calculated. All experiments have been performed in triplicate at 25°C using a Unico UV spectrophotometer. The BuChE inhibitory activity of the synthesized compounds was determined by using the same method and utilizing BTCh as substrate.

Docking study

Autodock Vina 1.1.1 was used for docking simulations [18]. The crystal structure of *Torpedo californica* acetylcholinesterase (1EVE) was retrieved through Protein Data Bank (http://www.rcsb.org/pdb/home/home.do). To prepare receptor and ligand for docking, the next procedure was conducted. Primary, the co-crystallized ligand along with water molecules was taken off the protein and the missing atom types were corrected. The atomic coordinates in the ligands were prepared employing Marvinsketch 5.8.3, 2012, ChemAxon (http://www.chemaxon.com) and the three-dimensional structures were obtained using Openbabel 2.3.1 [19]. Then, the receptor along with pre-optimized ligands was converted to required pdbqt structure using Autodock tools 1.5.4 [20]. The Autodock Vina variables were established as follows: box size: $15 \times 15 \times 15$ Å, the center of box: $x = 2.023$, $y = 63.295$, $z = 67.062$ (geometrical center of co-crystallized ligand), the exhaustiveness: 100, and the other variables remained unchanged. The obtained geometries were ranked regarding free energy of binding and the best positions were selected for additional analysis. All molecular visualizations were executed in DS Viewers Pro (Accelrys, Inc., San Diego, CA). To confirm the validity of our docking protocol, native ligand of enzyme was extracted and re-docked into the active site of enzyme. Applied docking protocol successfully reproduced the bound conformation of native ligand with a root-mean square deviation of 1.015 Å.

This work was supported by grants from the Iran National Science Foundation (INSF) and Research Council of Tehran University of Medical Sciences.

The authors have declared no conflict of interest.

References

[1] Y. Huang, L. Mucke, *Cell* **2012**, *148*, 1204–1222.
[2] Alzheimer's Association, *Alzheimer's Dement.* **2012**, *8*, 131–168.
[3] M. Prince, R. Bryce, C. Ferri, World Alzheimer Report 2011. Alzheimer's Disease International, London **2011**.
[4] K. Mullane, M. Williams, *Biochem. Pharmacol.* **2013**, *85*, 289–305.
[5] S. Thiratmatrakul, C. Yenjai, P. Waiwut, O. Vajragupta, P. Reubroycharoen, M. Tohda, C. Boonyarat, *Eur. J. Med. Chem.* **2014**, *75*, 21–30.

[6] W. Yang, Y. Wong, O. T. W. Ng, L. P. Bai, D. W. J. Kwong, Y. Ke, Z. H. Jiang, H. W. Li, K. K. L. Yung, M. S. Wong, *Angew. Chem. Int. Ed.* **2012**, *51*, 1804–1810.
[7] D. R. Howlett, A. R. George, D. E. Owen, R. V. Ward, R. E. Markwell, *Biochem. J.* **1999**, *343*, 419–423.
[8] L. Fang, X. Fang, S. Gou, A. Lupp, I. Lenhardt, Y. Sun, Z. Huang, Y. Chen, Y. Zhang, C. Fleck, *Eur. J. Med. Chem.* **2014**, *76*, 376–386.
[9] H. C. Kolb, K. B. Sharpless, *Drug Discov. Today* **2003**, *8*, 1128–1137.
[10] A. Tahghighi, S. Razmi, M. Mahdavi, P. Foroumadi, S. K. Ardestani, S. Emami, F. Kobarfard, S. Dastmalchi, A. Shafiee, A. Foroumadi, *Eur. J. Med. Chem.* **2012**, *50*, 124–128.
[11] Y. Bourne, H. C. Kolb, Z. Radic, K. B. Sharpless, P. Taylor, P. Marchot, *Proc. Natl. Acad. Sci. USA* **2004**, *101*, 1449–1454.
[12] A. Krasinski, Z. Radic, R. Manetsch, J. Raushel, P. Taylor, K. B. Sharpless, H. C. Kolb, *J. Am. Chem.* **2005**, *127*, 6686–6692.
[13] A. Shi, L. Huang, C. Lu, F. He, X. Li, *Bioorg. Med. Chem.* **2011**, *19*, 2298–2305.
[14] F. Himo, T. Lovell, R. Hilgraf, V. V. Rostovtsev, L. Noodleman, K. B. Sharpless, V. V. Fokin, *J. Am. Chem. Soc.* **2005**, *127*, 210–216.
[15] M. Meldal, C. W. Tornøe, *Chem. Rev.* **2008**, *108*, 2952–3015.
[16] Z. Jin, P Xue, E. Fu, *Synth. Commun.* **2014**, *44*, 6–75.
[17] M. Alipour, M. Khoobi, H. Nadri, A. Sakhteman, A. Moradi, M. Ghandi, A. Foroumadi, A. Shafiee, *Arch. Pharm. (Weinheim)* **2013**, *346*, 577–587.
[18] O. Trott, A. J. Olson, *J. Comput. Chem.* **2010**, *31*, 455–461.
[19] N. M. O'Boyle, M. Banck, C. A. James, C. Morley, T. Vandermeersch, G. R. Hutchison, *J. Cheminform* **2011**, *3*, 33.
[20] M. F. Sanner, *J. Mol. Graph. Model.* **1999**, *17*, 57–61.